In-vitro Assessment of Cone Beam Computed Tomography in the Detection of Fractures in the Vertical Plane

Aurelia Vanderburg

A thesis submitted to the faculty of the University of North Carolina at Chapel Hill in partial fulfillment of the requirements for the degree of Master of Science in the Department of Endodontics, School of Dentistry

Chapel Hill

2010

Approved by:

Advisor: Dr. André Mol. DDS, MS, PhD

Reader: Dr. Eric Rivera. DDS, MS

Reader: Dr. Asma Khan. BDS, PhD

ABSTRACT

AURELIA VANDERBURG

In Vitro Assessment of Cone Beam Computed Tomography For The Detection of Vertical Root Fractures
(Under the direction of Dr. André Mol)

The purpose of this study was to determine the accuracy of cone beam computed tomography (CBCT) for the detection of vertical root fractures (VRFs) in comparison to periapical radiography (PA). Fifty premolars and molars in dry skulls were accessed, instrumented and obturated. Fracture induction of twenty-one teeth took place using the Monaghan method. Three digital PAs with angular discrepancy of approximately 15 degrees and CBCT scans of each skull submerged in water, to simulate soft tissues, were made. All teeth were extracted and stained to obtain ground truth. Eight calibrated dentists determined VRF presence on a 5-point likelihood scale. **Conclusions:** PAs are more accurate than the CBCT for VRF detection. The specificity, positive likelihood ratio and diagnostic odds ratio are better for PA; there is no difference in sensitivity and negative likelihood ratio. Differences between the two modalities results from a high false positive rate associated with CBCT.

Special thanks to my committee, Dr. Sheng Zhong, the Endodontic and Radiology Residents in the completion and execution of this study.

Financial support was provided by the American Association of Endodontists (AAE) Foundation.

TABLE OF CONTENTS

LIST OF TABLES

Table

LIST OF FIGURES

Figures

LIST OF ABBREVIATIONS

2D	Two-dimensional
3D	Three-dimensional
ANOVA	Analysis of Variance
Az	Area under Receiver Operating Curve
CBCT	Cone Beam Computed Tomography
CCD	Charge-Coupled Device
CT	Computed Tomography
DICOM	Digital Imaging and Communication in Medicine
FPD	Flat Panel Detector
kVp	Kilovolt Peak
LCT	Local Computed Tomography
mA	Milliamperage
mm	millimeter
MPR	Multiplanar Reformatting
PA	Periapical Radiography
PDL	Periodontal Ligament
ROC	Receiving Operator Characteristic
SD	Standard Deviation
TACT	Tuned-Aperture Computed Tomography

VRF	Vertical Root Fracture

INTRODUCTION

Cracks and fractures of teeth pose a number of clinical challenges. Diagnosis is often difficult, resulting in uncertainty in treatment decisions. In addition, classification of cracks and fractures is not always standardized. A crack implies that an incomplete break in a tooth exists. A fracture implies that a complete or incomplete break in a tooth exists. When either a crack or fracture is present over a period of time along the long axis of a tooth, it is classified as a longitudinal fracture [1]. A longitudinal fracture can be observed within both the anterior and posterior dentition as a result of occlusal forces, dental procedures or both. Complex dental procedures can result in a substantial loss of enamel and dentin and increase the restoration-to-tooth structure ratio. This increases the risk of tooth cracks and fractures. With increasing life expectancy and more patients retaining their natural dentition, the incidence of longitudinal fractures is becoming higher. In addition, more patients are choosing complex dental treatment options in favor of extraction [2]. Detection of longitudinal fractures is difficult. Generally, detection is easier when they have been present for an extended period of time, when they become stained (naturally or iatrogenically), cause pain or cause bone loss. The techniques used to identify longitudinal fractures are: transillumination, biting devices (i.e. tooth sleuths), staining, magnification and radiography [3].

There have been five types of longitudinal fractures identified. From least to most severe, these are: 1) craze line; 2) fractured cusp; 3) cracked tooth; 4) split tooth; and 5) vertical root fracture (VRF) [2-4]. The aforementioned longitudinal fractures are often referred to as vertical root fractures. However, while a vertical root fracture (VRF) can be considered a longitudinal fracture, not all longitudinal fractures are VRFs [5-12]. Most of the studies in the dental literature focus on VRFs, leaving much to be desired with regard to our knowledge and understanding of craze lines, fractured cusps, cracked teeth and split teeth. The difficulty in identifying VRFs and the potential impact on treatment decisions has made the study of VRFs a priority in dental research. The following section is an overview of the different types of longitudinal fractures.

Craze Lines

Craze lines are very common within the permanent dentition. They only affect enamel and cause no pain [4]. When identified within the posterior dentition, they typically extend to the marginal ridges and along the buccal and lingual surfaces. When craze lines are observed within the anterior dentition, they usually extend from the cervical area to the incisal edge and may be of esthetic concern. Craze lines occur routinely and are not considered precursors to dentin fractures [3-4].

Fractured Cusp

A fractured cusp is defined as a complete or incomplete fracture that initiates from the crown of a tooth and extends subgingivally in both the mesio-distal and facial-lingual orientations to the cervical third of the crown or root (Figure 2) [2-4, 13,14]. Typically, the marginal ridges and facial or lingual grooves are involved[5,15]. When observed clinically, one or two cusps may be involved. A single cusp fracture includes the mesio-distal and facial-lingual components. A two-cusp fracture involves the mesial and distal components without the facial-lingual components. The most common causes of fractured cusps are large restorations and extensive decay [16]. Extensive loss of sound dentin through decay or large restorations can result in undermined and unsupported tooth structure, which increases the tooth's susceptibility to fracture [17]. Cuspal fractures tend to be shallow and as a result very rarely directly affect the pulp. However, patients may experience cold sensitivity and sharp pain on mastication when this type of fracture is present. Cold testing to determine pulp vitality and biting tests with the tooth sleuth or cotton swab applicator are used to confirm the presence of a cusp fracture. Treatment of a fractured cusp typically involves the placement of a three-quarter or full-coverage crown that extends below the most apical portion of the fracture. A fractured cusp is almost always removed unless it is non-mobile. When the fractured segment is non-mobile it is included within the permanent restoration. The long term prognosis for a tooth with a fractured cusp is generally good unless the fracture extends significantly beyond the gingival attachment in which case permanent restoration is difficult [14].

Cracked Tooth

A cracked tooth is a variant of a fractured cusp (Figure 3). The difference is that the fracture of a cracked tooth is centered occlusally and extends more apically than a fractured cusp [6-8]. The formal definition of a cracked tooth is that it is an incomplete fracture that initiates from the

crown and extends subgingivally in the mesio-distal direction [3-4, 18-20].

In a cracked tooth, one or both of the marginal ridges and proximal surfaces may be included. Most cracked teeth are identified in elderly patients and include first and second mandibular molars or maxillary second molars and premolars [18, 20-23]. Biting on a hard or brittle substance is the most common cause of a cracked tooth [4]. It has also been hypothesized that teeth may crack when dentin cracks and weakens in heavily restored teeth in response to the stress between the expansion and contraction of the restorative material and tooth structure. Various signs and symptoms characterize a cracked tooth [9]. A patient with a cracked tooth may experience sharp non-lingering pain when biting, when taking cold foods and beverages, or even spontaneously. When performing diagnostic tests, a patient with a cracked tooth may have severe to moderate pain to percussion (directional percussion tests not directed along the long access of a tooth) or during a biting test (biting on tooth sleuth). In addition, bone loss may be observed, either horizontal, vertical or in the furcation [2], which may be identified clinically by deep isolated probing depths. However, the best way

to detect a cracked tooth is by direct visualization. If a tooth is unrestored and a crack is observed, it is advised that the crack be traced with a handpiece to determine its extent and subsequent restorability of the tooth. If a tooth is restored, stepwise dismantling including methylene blue, transillumination and magnification are advised in the management of a crack [24]. After complete removal of a restoration in a restored tooth [25], visual inspection should take place with and without the microscope followed by transillumination or methylene blue dye to identify any cracks. If a crack is identified, it should be followed with a handpiece to determine its extent and restorability of the tooth in question. If a crack extends extensively beyond the crestal bone and involves the pulp, the prognosis is poor and extraction is usually required. If a cracked tooth involves the pulp but does not extend below the crestal bone, the prognosis is good and non-surgical root canal treatment with full coverage restoration is advised. The prognosis for a cracked tooth decreases from questionable to poor when cracks involve: (1) one marginal ridge limited to the crown; (2) two marginal ridges limited to the crown; (3) marginal ridge(s) and internal proximal cavity wall only; (4) marginal ridge(s) and floor cavity preparation; (5) one marginal ridge extending from the crown to the root surface; (6) two marginal ridges extending from the crown to the root surface; (7) marginal ridge(s) and into canal orifice(s); (8) marginal ridge(s) and pulpal floor [2-3]. In general, the prevalence of cracked teeth can be decreased when full coverage restorations are used instead of large class I and class II restorations in the posterior dentition [26].

Split Tooth

Over time, a cracked tooth may develop into a split tooth [2-4]. A split tooth is a complete fracture that initiates in the crown and extends to the root subgingivally in a mesio-distal direction through both marginal ridges and proximal surfaces of a tooth (Figure 4). It is diagnosed by visual separation of two tooth segments mesio-distally with wedging forces and is often associated with deep isolated probing depths mesio-distally [2, 10-11, 27].

The cause of a split tooth is persistent wedging or a displacement force on an existing restoration or an acute traumatic force that exceeds the elastic strength of dentin in a restored tooth. A patient with a split tooth often presents with an abscess and pain on biting. Radiographically, the fracture line of a split tooth cannot be visualized because of its mesio-distal orientation. However, bone loss can be observed radiographically as an indication of a split tooth. The only treatment option for a split tooth is extraction as it has a poor prognosis. Split teeth can be prevented by using conservative endodontic access preparations and the elimination of oral habits that impose wedging forces on heavily restored dentition [28].

Vertical Root Fracture

A true vertical root fracture (VRF) is defined as a complete or incomplete fracture initiated in the root at any level, usually directed buccolingually (Figure 5) [1-3, 12, 29-37]. A VRF most commonly occurs within the maxillary second premolar (27%) and the mesial roots of the mandibular molar (24%). [32] Vertical root fractures occur slightly more often in

women (52%) than in men (47%) and are more common in individuals between the ages of 41 and 50 [15]. The prevalence of VRF in the general population is between 2% and 5%. [32]. Various factors have been found as causative or contributing factors in the development of a VRF. Physical trauma, occlusal prematurity, repetitive heavy and stressful chewing, resorption-weakening and iatrogenic dental treatment have all been mentioned as factors in the development of a VRF. However, the most common dental procedure to cause a VRF is overzealous endodontic treatment, including excessive canal shaping and excessive pressure during compaction of gutta-percha [15, 31, 33, 38-42]. A study conducted by Fuss and coworkers in 2006 found that dowel placement results in VRF production 67% of the time [38-39, 41-44].

Clinically, VRFs are associated with specific signs and symptoms. The most common signs and symptoms are: pain to percussion (69%), pain to palpation (69%), pain when chewing (61%), mobility (61%), swelling (15%), sinus tract (18%), an isolated periodontal defect (40%), and a halo or J-shaped radiolucency (36%).[15, 32, 35, 39, 42, 45-46] Patients typically display these signs and symptoms when extensive propagation of the fracture has taken place. Treatment options for teeth diagnosed with a VRF vary, however, the prognosis of a tooth with VRF is generally poor and extraction is usually the treatment of choice. In multi-rooted teeth, a hemisection or radisectomy could be performed if the VRF is localized [27, 47]. The diagnosis of a VRF is very difficult and relies heavily on a patient's comprehensive dental history, analysis of the patient's symptoms and radiographic analysis [32]. Currently, periapical radiographs are used to determine whether a VRF is present.

Clinicians check for the presence of a fracture as well as for a halo sign or periodontal lesions that occur in 28-36% of teeth with VRF. Actual radiographic visualization of a VRF is difficult and inconsistent and is only possible when the x-ray beam is parallel to the fracture line and adjacent anatomical structures do not overlap [48].

Visualizing a VRF using conventional transmission radiography requires the production of detectable contrast between the fracture and the surrounding tooth structure, which is only produced when the plane of the fracture and the orientation of the x-ray beam coincide. The acquisition of multiple intra-oral radiographs using different angles certainly increases the probability of fracture detection; however, the three-dimensional nature of the object makes detection uncertain. A number of investigators have studied the possibility of using three-dimensional radiographic imaging for the detection of VRFs [49-52]. A number of studies have assessed the accuracy of computed tomography for the detection of VRFs. Computed tomography is a three-dimensional imaging technique that uses image reconstruction to produce tomographic images [53]. Medical computed tomography (MDCT) scanners consist of an x-ray source producing a fan-shaped x-ray beam and a detector. The x-ray source and the detector rotate around a gantry through which the patient is moved during image acquisition. This creates a spiral image set which can be reconstructed into an image volume.

Youssefzadah and co-workers conducted a study in 1999 in which the accuracy of conventional periapical radiographs was compared to medical CT scans in the early detection of VRFs[49]. Thirty-seven patients with endodontically treated posterior and anterior teeth with clinical indications of a VRF were utilized in this study. Each patient obtained a periapical radiograph of the affected dentition and a computed tomography scan of their head. Two radiologists viewed all of the images and ground truth was obtained via an exploratory surgery where the tooth in question was viewed under magnification and stained with methylene blue. Diagnostic accuracy was measured in this study in terms of specificity and sensitivity. Medical CT (75%) was found to be superior to conventional dental radiography (25%) in the detection of vertical root fractures within this study [49]. While the modalities analyzed within this study are clinically relevant, the use of MDCT for dental purposes is unrealistic because of cost and dose.

In 2001, Nair and co-workers conducted a study comparing the accuracy of digital radiography, Tuned-Aperture Computed Tomography (TACT), and iteratively restored TACT in the detection of VRFs. Fifty-four single rooted mandibular teeth in ten cadaveric mandibles were used in this study. All teeth were accessed, instrumented, obturated and prepared for a post space. Fractures were created in 28 teeth using the Monaghan method and the remaining 26 teeth were left intact. Images were created of the teeth with the three modalities analyzed within this study and eight observers participated in viewing sessions. A 5-point response scale was used for fracture determination and ROC analysis was used to

determine the accuracy between the three radiographic modalities. Additional measures of sensitivity and specificity were also assessed. Ground truth was obtained by extracting all teeth and visualization of the teeth with transillumination. The most accurate radiographic modality in the detection of VRFs within this study was TACT [48]. Although the use of TACT is possible in clinical practice, its use requires considerable effort, making its routine use for unrealistic.

Mora and coworkers conducted an *in-vitro* study in 2007 comparing the accuracy of local computed tomography (LCT) and conventional periapical radiographs in the visualization of VRFs[51]. Sixty endodontically accessed extracted teeth were utilized in this study. Fracture induction took place using the Monaghan method in a controlled environment where the teeth were mounted in acrylic blocks. Scanning of the samples took place with the teeth mounted in a dry mandible with boxing wax and grains to simulate trabecular bone and soft tissue. LCT scans and periapical radiographs were obtained of all samples. Ten calibrated observers viewed the images and recorded their responses on a 5-point response scale. ROC analysis was used to determine the diagnostic accuracy of both modalities. It was found that LCT significantly improved the detection of VRFs when compared to conventional periapical radiology [51].

In 2005, Hannig and co-workers conducted an *ex vivo* study in which they compared a flat panel volume detector computer tomography system (FD-VCT) to conventional periapical

radiography for the detection of VRFs. Five patients with endodontically treated teeth that presented with signs and symptoms of VRF were utilized in this study. Periapical radiographs were obtained of each tooth in question prior to extraction. Following extraction, periapical radiographs and FD-VCT scans were taken of the extracted tooth. This pilot study showed that FD-VCT can be used to clearly visualize vertical root fractures [50]. Although the fact that the teeth were imaged following extraction reduces the clinical significance of the study.

Cone-beam computed tomography (CBCT) was first introduced in 1982 for angiography.[53-54] Within the literature, CBCT has been referred to as dental volumetric tomography, cone-beam volumetric tomography, dental computed tomography and cone beam imaging. The shape of the x-ray beam is either conical or pyramidal, depending on the type of detector used. Cone-beam CT imaging involves a single half or full rotation around the patient [55]. At small intervals, single projection images, known as basis images, are acquired. Specific software programs reconstruct the basis images into a 3D volumetric data set that can be reconstructed into axial, sagittal, coronal or custom planes [55]. During image acquisition, a patient may be seated, standing or supine, depending on the type of scanner [53]. Regardless of the position, the patient's head should be immobile. Any movement during a scan will decrease the quality of the final image. Supine CBCT units take up a large surface area and are not easily accessible for patients that are physically impaired. Seated CBCT units are the

most comfortable but may not accommodate wheel chair bound patients. Standing units are the most common, but height adjustment is difficult for patients that are wheel chair bound. The selection of technique factors, if controlled by the operator, should be based on ALARA (As Low As Reasonably Achievable) [53, 56]. Based on the size of the patient, the current (mA) and voltage (kVp) should be adjusted to values that emit the lowest amount of radiation necessary to produce a diagnostic image. Some CBCT units automatically adjust mA and kVp values for each patient via a process referred to as automatic exposure control. During this process kVp and mA are automatically modulated in real time by a feedback mechanism in which the intensity of the transmitted radiation is detected. A second method automatically adjusts radiation exposure in CBCT units after recording readings obtained during the initial scout exposure scan. This method of exposure adjustment is greatly desired because it does not require operator input.

Field of view determines the size of the image volume and is an important parameter in the selection of a CBCT scanner. Most units have a fixed field of view; however, some manufactures are now producing units that can accommodate multiple fields of view. The field of view is affected by the detector size and shape, the beam projection geometry and the limits of beam collimination. The shape of the scan volume can be cylindrical or spherical. Collimation of the x-ray beam restricts x-radiation exposure to the region of interest. CBCT units can be divided into two groups on the basis of detector type: those that use an image intensifier (II) in combination with a charge-coupled device (CCD) and those that use a flat-

panel detector. The II/CCD detector contains an x-ray image intensifier tube coupled to a charge-coupled device with fiber-optic coupling. A flat-panel detector uses a large area solid-state sensor panel coupled to an x-ray scintillator layer [56]. The most common flat-panel configuration consists of a cesium iodide scintillator applied to a thin film transistor made of amorphous silicon[53, 56].

The pixel size of an area detector determines the voxel dimensions in a CBCT image volume. The spatial resolution of CBCT is determined by the individual volume elements or voxels produced from the volumetric data set. The resolution of the area detector is submillimeter (0.09 mm to 0.4 mm) and this primarily determines the size of the voxel [56]. Most CBCT units provide isotropic voxels[53, 56].

Once basis images have been acquired, primary reconstruction takes place where all of the basis images are combined to create a volumetric data set. The volumetric data set is the final radiographic image that is utilized and can be manipulated for diagnostic purposes. The reconstruction of basis images into a volumetric data set is computationally complex and requires a personal computer. The ideal time frame for image reconstruction is less than 5 minutes. Short time frames complement patient flow. Reconstruction time depends on the acquisition parameters (voxel size, size of the image field, and number of projections), hardware (processing speed, data throughput) and software (reconstruction algorithms) being used. In general, the final data set is initially presented to the clinician in three orthogonal

planes (axial, sagittal and coronal). Optimal visualization of the final data set is obtained by the adjustment of window level and window width to favor bone and the application of specific filters[53].

Advantages of CBCT

The use of CBCT technology in the field of dentistry provides several advantages in the imaging of the maxillofacial region.

Reduced patient radiation dose

When comparing radiation exposure from a CBCT scan to that of a conventional medical CT scan, patient radiation dose is 98.5% to 76.2% less for a CBCT scan [56-59]. The effective dose for CBCT, which represents the total biologic detriment based on the tissues being exposed and the tissue sensitivity, has also been compared to the effective dose of panoramic radiography and to background radiation. The dose from CBCT is equivalent to 2-35 times that of a single exposure for a panoramic radiograph, depending on the type of scanner being used. The number of days of equivalent background radiation varies between 3 to 48 days [56]. The field of view, technique factors, number of basis images and the tissues exposed during image acquisition are some of the main variables determining the effective dose.

Image accuracy

Image volumes produced by CBCT technology generally consist of isotropic voxels ranging from 0.4 mm to 0.076 mm [56]. This provides a spatial image resolution that is similar to or

better than the spatial resolution of panoramic radiography. The accuracy of measurements within the volume is high and meets the needs of most clinical applications.

Image reconstruction

The isotropic voxels of the image volume assures consistent spatial resolution of any type of image reconstruction. Multiplanar reformatting (MPR) enables the clinician to view orthogonal images in the axial, coronal and sagittal planes [56]. Other types of representations of the volumetric data sets include panoramic layers, ray sum images to simulate cephalometric projections and volume and surface rendered images.

Disadvantages of CBCT

CBCT technology has limitations related to the "cone-beam" projection geometry, detector sensitivity and contrast resolution. The clarity of CBCT images is affected by artifacts, noise, and poor soft tissue contrast.

Artifacts

The formal definition of an artifact is any distortion or error in an image that is unrelated to the subject being studied [56]. Classification of artifacts is based on their cause.

Cone beam-related artifacts

Three types of cone-beam related artifacts are produced as a result of the projection beam geometry of the CBCT and the image reconstruction method: (1) partial volume averaging; (2) undersampling;(3) cone-beam effect [56]. Partial volume averaging takes place when the selected voxel resolution of the scan is greater than the spatial or contrast resolution of the subject to be imaged. Selection of small acquisition voxels reduces the presence of this type of artifact [56].

Undersampling takes place when too few basis projections are obtained for reconstruction. When this artifact is present, misregistration, sharp edges, noise or fine striations can be seen in the final image. This artifact reduces the fine detail of a final image [56]. Cone-beam effect artifacts produce final images that are distorted, having greater peripheral noise and streaking. These features are produced as a result of a lack of radiation exposure of the peripheral aspects of the subject being scanned. This artifact is minimized by various forms of cone-beam reconstruction being incorporated into the CBCT units being manufactured [56]. Clinically, this artifact can be reduced by positioning the region of interest adjacent to the horizontal plane of the x-ray beam and collimation of the beam to the appropriate field of view.

X-ray beam artifacts

This type of artifact is the result of beam hardening which takes place as a result of the polychromatic nature of the x-ray beam. In beam hardening the lower energy photons are absorbed more readily than the high energy photons and this causes the overall energy of the

x-ray beam to increase. The two types of artifacts that are produced as a result of beam hardening are: (1) Distortion of metallic structures due to differential absorption, also known as cupping artifact; (2) streaks and dark bands that can appear between two dense objects [56]. To prevent these artifacts, beam collimation, modification of the patient's position or separation of the dental arches can take place to reduce the field of view. CBCT manufactures have also added an artifact reduction technique algorithm within the reconstruction process in an effort to prevent beam hardening.

Patient-related artifacts

Movement by the patient during a scan cycle and the presence of metallic objects in the patient produce artifacts that decrease the diagnostic quality of the final image. Movement during scanning causes misregistration of data that visually presents as unsharpness in the final reconstructed images. Short scan times and head restraint devices minimize patient motion artifacts. Metallic objects cause horizontal streaks in the final images as discussed in the section on x-ray beam artifacts. Patients should remove all removable metal items that are located in the field of view prior to CBCT image acquisition.

Poor soft tissue contrast

The use of a cone-beam implies that a large proportion of x-ray attenuation will produce scatter radiation. A large number of scattered x-ray photons will reach the detector. These

photons do not contribute to the actual image and reduce image contrast. This is the main reason why cone-beam CT scanners show poor soft tissue contrast.

Applications of CBCT

CBCT imaging is currently being used within the field of dentistry for implant site assessment, dental pathologic conditions, fracture assessment, craniofacial deformities, temporomandibular joint assessment, 3D cephalometry (orthodontics) and growth and development[55-56]. In addition to its diagnostic capabilities, CBCT is also being used to facilitate guided surgeries. Software is now available that provides surgical simulations for osteotomies and distraction osteogenesis. Diagnostic and planning software is also available that assists in orthodontic assessment and analysis and in implant planning to fabricate surgical models, surgical stents and drill guides [56].

Several studies have been conducted to assess the accuracy of CBCT for the detection of VRFs as compared to conventional periapical radiographs. In 2009, Hassan and co-workers compared conventional periapical radiography to cone beam computed tomography (CBCT) using eighty extracted human teeth [60]. All teeth were accessed, instrumented and decoronated. Half of the sample was obturated with gutta-percha and fractured under controlled conditions using the Monaghan method. All samples were placed in premade sockets in a dry human mandible, which was coated with three layers of dental wax to simulate soft tissue. The I-CAT was used for CBCT imaging and two periapical images were

made of each sample: one straight and one with a more mesial angle. Four calibrated observers viewed all of the images and recorded their responses on a dichotomous scale. Accuracy between the two modalities was determined by sensitivity and sensitivity statistical tests [60]. CBCT was found to be more accurate than periapical radiographs in the visualization of VRFs. A more recent study conducted by Hassan in 2010 compared five different CBCT units for the detection of vertical root fractures [61]. Using similar materials and methods, images were obtained of all samples using five CBCT systems. Two calibrated observers viewed all of the images and recorded their responses on a dichotomous scale. They concluded that (1) root canal filling (gutta percha) reduced the specificity of all CBCT units and (2) root canal filling influenced four out of five units' accuracy [61].

The purpose of the current study is to determine the accuracy of one commonly used CBCT scanner (Sirona Galileos Comfort) for the detection of VRFs in comparison with multi-angle periapical radiography. The experimental design was chosen to reflect as closely as possible the current clinical environment while maintaining access to the actual status of the roots. This study addresses a well-defined and urgent clinical dilemma. If CBCT were found to be more accurate than conventional periapical radiography in detecting VRFs, it could become a standard procedure in endodontics.

MATERIALS AND METHODS

An *in-vitro* model was used, consisting of three dry skulls (Figure 8) with fifty available human posterior teeth. First and second premolars and first, second and third molars from all four quadrants were utilized in this study. Twenty-one teeth were randomly selected to be vertically fractured, while the remaining twenty-nine teeth served as controls and remained non-fractured (Table 1). For all the teeth, endodontic access openings (Figure 9) were made and the canals were located, shaped, and obturated.

All fifty teeth were accessed utilizing a high speed handpiece and coolant with a 4-round carbide surgical length and Endo-Z bur. Upon access completion, canals were located with an endodontic explorer and ethylenediaminetetraacetate (EDTA) in calcified cases. Shaping of the canals took place utilizing the K3 and Sequence Rotary System in a crown down technique. K3 nickel titanium rotary files were used to instrument the middle and coronal third of the root. Sequence nickel titanium rotary files were used to instrument the apical third of the roots. The apical third of each canal was instrumented to a master apical file size ranging from 35.04- 45.04; three sizes larger than the first file size to bind dentin at the working length. [32], [34].

Fracture induction within the twenty-one experimental teeth took place within the oral cavity of the dry skulls. A stiff 60-degree beveled tip conical wedge (Figure 12) was fitted within 2-3mm of the measured working length [62]. It was then marked with an endodontic rubber stop 1 mm short of the working length. A surgical mallet with an approximate weight of 500

g (Figure 11) was used to strike the conical wedge to the working length marked by the endodontic rubber stop [32]. Canals of both the fractured and non-fractured dentition were obturated with .04 tapered Resilon cones. Sponges were placed over the obturated canal orifices and the accesses were restored with Cavit.

Image Acquisition

Cone-beam CT scans were obtained of all three skulls using the Sirona Galileos Comfort (Figure 6, Figure 7) scanner (Sirona Dental Systems GmbH, Bensheim, Germany). To simulate soft tissue, each skull was submerged in water during each CBCT scan [63]. The Galileos unit was set to 85kV and 42mAs under the V01 setting. The Galileos scanner produces a standard isotropic voxel size of 0.3 mm. Close-up images of individual teeth were generated following image acquisition. The close-up views unbind the standard voxels and provides the native 0.15 mm voxel size. The close-up volumes were exported in the Digital Imaging and Communication in Medicine (DICOM) format for viewing in third party software (InVivoDental by Anatomage, San Jose, CA).

Conventional intraoral periapical radiographs were obtained with a Kodak RVG 6000 sensor (Eastman Kodak Company, Rochester, NY); using a Sirona intraoral x-ray source. The Rinn system was used to stabilize the sensor within the oral cavity of all the dry skulls. Posterior maxillary teeth were exposed at 0.10s. Posterior mandibular teeth were exposed at 0.06s.

Each tooth exposed straight-on and at horizontal mesial and distal angles that varied by approximately 15 degrees.

Observation Sessions

Eight observers were recruited for this study. The group consisted of three third-year radiology residents, one endodontic faculty member, two second-year endodontic residents, and two third-year endodontic residents. Each observer had at least four years of dental education and participated in a calibration session prior to observation. The calibration sessions consisted of viewing periapical radiographs and CBCT scans that contained images of fractured and non-fractured teeth. The calibration images of fractured teeth displayed fractures that were on the root surface beneath the crestal bone. CBCT images were viewed using InVivoDental software and the observers were trained on how to manipulate and navigate the images with this program The choice of InVivoDental software over the native Sirona Galaxis software was based on the fact that the InVivoDental software allowed reorientation of the volume in every dimension. A basic instruction sheet was provided with directions on image navigation. Observers were also informed that the sagittal view always appeared to the observer as the right side of the patient. The observers were encouraged to browse through the axial, coronal and sagittal slices and to adjust the orientation of the volume according to the orientation of the long axis of the root to be examined. The study sample images were coded and randomized. Half of the observers viewed the CBCT images first, the other half viewed the conventional radiographs first. All CBCT images and

periapical radiographs were viewed on a 21.3 inch true color flat panel monitor with a resolution of 1600x1200 pixels under dim ambient lighting. All conventional radiographic images were observed in a PowerPoint presentation with the three projections of each tooth displayed side by side against a gray background. When viewing the images, the observers were asked to assess whether or not a longitudinal fracture was present and to record their response on a 5-point probability scale: 1= fracture is definitely not present; 2=fracture is probably not present; 3=unsure; 4=fracture is probably present; and 5=fracture is definitely present.

Ground Truth

Following radiographic observation and analysis, each sample (control and experimental) was carefully removed from the oral cavity of the dry skulls and stained with 1% methylene blue. The dye was placed upon the entire root surface of each tooth (Figure 13). The presence or absence of longitudinal fractures was assessed visually by a single investigator. If a longitudinal fracture was observed, its orientation and location were noted.

Statistical and Data Analysis

Based on observer responses, receiver operating characteristic (ROC) curves were created for each observer and modality with the ROCKIT software (Version 0.9, Charles E Metz, The University of Chicago, and Chicago, IL). Analysis of variance was used to test for differences between the areas under curves (A_z) as main effects of modality and observer as

well as their interaction. Raw ROC scores were also converted to dichotomous values in order to calculate other measures of diagnostic accuracy, including sensitivity, specificity, positive likelihood ratio (LR+), negative likelihood ratio (LR-) and diagnostic odds ratio (DOR). These additional measures of diagnostic accuracy were calculated to gain more insight in the observers' responses and the performance of the two modalities. The ROC responses were dichotomized by considering a score of 1, 2, or 3 as a negative response (no fracture) and scores 4 and 5 as a positive response (facture present). The dichotomized responses were used to assess the true positive rate (sensitivity), the true negative rate (specificity), the ratio between the proportion of fractured teeth with a positive response and the proportion of non-fractured teeth with a positive response (LR+), the ratio between the proportion of fractured teeth with a negative response and the proportion of non-fractured teeth with a negative response (LR+), and the overall discriminative power of the modalities (DOR).

Analysis of variance (ANOVA) was utilized to determine if there was a significant difference between the observers and between the two modalities with regard to the A_z-values, sensitivity specificity, LR+, LR- and DOR. All alpha levels were set at 0.05. The null-hypothesis of no difference regarding the detection of vertical root fractures between the modalities and the observers was tested for each of the outcome measures.

RESULTS

ROC Analysis

Table 2 shows the individual A_z-values for each observer and each modality. The mean A_z-value for periapical radiography was 0.70 (SD 0.07) and the mean A_z-value for CBCT was 0.58 (SD 0.08). This difference was statistically significant (ANOVA: $p = 0.0134$). The difference between the observers was not statistically significant (ANOVA: $p = 0.3307$). Figure 1 is a visual representation of the data contained in Table 2 based on pooled observer data. The area beneath the periapical radiography curve is greater than the area beneath the CBCT curve.

Sensitivity

Table 3 shows the sensitivity values for each observer and each modality. This measure represents the true positive rate, i.e. the percentage of fractured teeth correctly detected. The mean sensitivity for periapical radiography was 0.54 (SD 0.10). The mean sensitivity of CBCT was 0.60 (SD 0.19). The difference between the modalities was not statistically significant (ANOVA: $p = 0.3445$), nor was the difference between the observers (ANOVA: $p = 0.1360$).

Specificity

Table 4 shows the specificity values for each observer and each modality. This measure represents the true negative rate, i.e. the percentage of non-fractured teeth correctly identified. The mean specificity of periapical radiography was 0.72 (SD 0.10) and the mean specificity of CBCT was 0.49 (SD 0.15). The difference between the modalities was statistically significant (ANOVA: $p = 0.0048$), whereas the difference between the observers was not statistically significant (ANOVA: $p = 0.3181$).

Positive Likelihood Ratio

Table 5 shows the positive likelihood ratio (LR+) for each observer and each modality. The mean LR+ for periapical radiography was 2.16 (SD 0.71) and the mean LR+ for CBCT was 1.19 (SD 0.31). The difference between the modalities was statistically significant (ANOVA: $p = 0.0139$), and the difference between the observers was not (ANOVA: $p = 0.6839$).

Negative Likelihood Ratio

Table 6 shows the results for the negative likelihood ratio (LR-) for each observer and both modalities. The mean LR- value for periapical radiography was 0.63 (SD 0.11) and the mean LR- value for CBCT was 0.80 (SD 0.27). The difference between the modalities was not

statistically significant (ANOVA: p = 0.1286), nor was the difference between the observers (ANOVA: p 0.1286).

Diagnostic Odds Ratio

Table 7 shows the results of the diagnostic odds ratio (DOR) values for each observer and both modalities. The mean DOR value for periapical radiography was 3.52 (SD 1.23) and the mean DOR value for CBCT was 1.77 (SD 0.97). The difference between the modalities was statistically significant (ANOVA: p = 0.0189), and the difference between the observers was not (ANOVA: p = 0.5871).

DISCUSSION

A true vertical root fracture is a complete or incomplete fracture that initiates at any level of the root in a bucco-lingual orientation. VRFs most commonly occur within the maxillary second premolar and the mesial root of the mandibular molar [32]. The etiology includes post placement, obturation and excessive root-dentin removal. The most common signs and symptoms of a vertical root fracture are pain to percussion, pain to palpation, pain when chewing, mobility, swelling, sinus tract, an isolated probing depth, and a "halo" radiolucency (J-shaped) radiographically. Patients typically display the signs and symptoms of a vertical root fracture when extensive propagation of the fracture has taken place. The presence of a VRF often means a poor prognosis and imminent extraction of the effected tooth. Diagnosis of a VRF is very challenging and currently relies on patient's symptoms, dental history and periapical radiographic analysis. Determining the presence or absence of a VRF based on periapical radiography is difficult and inconsistent because actual visualization of a VRF can only occur when the x-ray beam is parallel to the fracture line and adjacent anatomical structures do not overlap. Given this difficulty, various studies have been conducted to investigate alternatives to conventional intra-oral radiography, including computed tomography, tuned-aperture computed tomography, local computed tomography and cone-beam computed tomography (CBCT). CBCT is of interest because it delivers accurate three-dimensional information at a relatively low cost and low dose. The compact design of CBCT units further enhances its potential for clinical usage within the dental office. Previous

studies that have compared conventional periapical radiography to CBCT in the visualization of VRFs have found CBCT to be more accurate than periapical radiography. The purpose of this study was to compare digital periapical radiography to a common CBCT scanner (Sirona Galileos) for the detection of VRFs. In this study Resilon was used as the obturation material.

The aims in designing this study were to develop a model that utilized a common CBCT unit, create a study model that enabled access to the ground truth and to create a model that resembled clinical conditions as closely as possible. To date, the only studies that have looked at CBCT in the detection of VRFs are the studies conducted by Hassan. The 2009 Hassan study only utilized the I-CAT scanner, but the 2010 study included the NewTom 3G, Galileos 3D, Scanora 3D, 3D AccuiTomo-xyz, and the Next Generation i-CAT . While Hassan found the Galileos unit to be the least accurate of the units analyzed within his studies, it was used in this study, in part because it was available for the study and in part because it is one of the more popular scanners being sold in the United Sates. Only the Youssefzadeh study conducted in 1999 utilized an *in-vivo* model. Patients suspected of having a VRF as a result of clinical signs and symptoms underwent medical CT scanning for fracture detection and a surgery with methylene blue staining to obtain ground truth. Previous studies by Hassan, Mora, Nair and Hannig utilized an *in-vitro* model where teeth were scanned and extracted (Hannig study) or used a cadaver mandible coated with dental wax bucco-lingually. Youssefzadeh's model is the most ideal, but with an *in-vitro* model the sample size and experimental conditions can be better controlled. Like most previous

studies, an *in-vitro* model was used in this study in order to obtain the ground truth. Soft tissue simulation took place in this study with skull submersion in water. Dental wax was not used for soft tissue simulation in this study because of the large surface area of the dry skulls. All of the samples in this study contained a root canal filling. The root canal filling used in this study was Resilon. All previous studies used gutta-percha as the root canal filling. This is the first study to use Resilon as the root canal filling in the evaluation of VRF teeth. The Hassan studies decoronated the sample teeth to eliminate fracture detection in the enamel. The access cavities were closed with Cavit to avoid coronal fracture detection within this study. Slight detection of fractures coronally with Cavit in the access was possible in a small number of the periapical radiographs of this study. This may have created a bias within this study. The Hassan studies also used magnification to visually inspect the sample teeth for VRFs prior to utilization within the study. Teeth were only inspected for iatrogenic fractures within this study after radiographic scanning. It was confirmed that only the teeth that were purposefully fractured had vertical root fractures in the buccolingual orientation. Extensive displaced vertical root fractures were created or present in all previous studies, whereas the fractures in this study were not displaced and varied in extent. Observers only relied on visual observation to denote the presence of a VRFs in this study. The observers in the Youssefzadeh study were aware of each patient's clinical signs and symptoms. This may have created a bias in the observer's radiographic evaluation. All previous studies also used digital periapical radiography. The 2009 Hassan study is the only study that used two angled periapical radiographs. In addition to clinical signs and symptoms, VRFs are diagnosed

radiography as a result of the pathology associated with VRFs radiographically. Viewers were given three angled radiographs of each sample within this study. These are not traditional clinical conditions and it can be said that this created bias in favor of periapical radiography in this study. In summary, the experimental design of the current study was unique in that because of the use if one CBCT unit and three angled periapical radiographs and the fact that the teeth were coronally filled with Cavit and contained Resilon as the root canal filling material.

Based on the ROC A_z-values, it was shown that periapical radiography was significantly more accurate than CBCT for the detection of VRFs. This result is different from previous studies where CBCT was found to be more accurate than conventional periapical radiography in the visualization of VRFs, although these studies only utilized sensitivity and specificity tests to determine the accuracy of the two modalities (Hassan 2009). Following dichotomization of the ROC scores it was shown that the two modalities were not different in terms of their sensitivity. In fact, CBCT had a slightly higher mean sensitivity than periapical radiography, but this difference was not statistically significant. On the other hand, the specificity of periapical radiography was significantly greater than the specificity of CBCT. This implies that CBCT resulted in a higher false positive rate than periapical radiography. Potential causes for the increased false positive rate with CBCT include the presence of radiolucent lines and streaks as a result of beam hardening or undersampling. The presence of beam hardening artifacts may have been more prominent in this study because of the higher x-ray absorption of Resilon compared to that of gutta-percha. Resilon contains

radioopaque fillers in addition to barium sulfate within its makeup whereas gutta-percha only contains barium sulfate. In addition, the Sirona Galileos limited sampling rate may have caused additional streaking or enhanced existing beam hardening artifacts. The mean specificity values for the 2009 and 2010 studies by Hassan and co-workers using gutta-percha were 0.87 and 0.85, respectively. These specificity values are higher than the specificity values obtained for CBCT in this study. Although the mean specificity value for periapical radiography was higher than for CBCT, it is still considered relatively low (0.72). This implies that periapical radiography also results in a number of false positive assessments in addition to a low true positive rate. While the difference in the mean sensitivity values of periapical radiography and CBCT are not statistically significant, both values are low. For periapical radiography, a mismatch between the orientation of the x-ray beam and the orientation of the fracture seems the most plausible explanatory variable. Insufficient contrast and overlap of anatomical structures may also contribute to reduced visualization of fractures. For CBCT, the low sensitivity value cannot be explained by unfavorable projection geometry: image slices can be reconstructed from the image volume in any orientation and location. Thus, other factors limit the sensitivity of the Sirona Galileos CBCT scanner in detecting VRFs. One of these factors could be insufficient spatial resolution. The maximum spatial resolution is determined by a number of factors, including voxel size, contrast, noise and the presence of artifacts. Although the native voxel size of 0.15 mm may appear adequate for the detection of non-displaced fractures, the voxel size represents a theoretical upper limit to the spatial resolution, but by no means represents the actual maximum

resolution of the imaging system. The contrast resolution and the presence of noise and artifacts are some of the factors that reduce spatial resolution. While the true spatial resolution of the Galileos image volume is not known, the results of this study suggest that it was close to or less than the spatial resolution required for fracture detection

The positive and negative likelihood ratios and the diagnostic odds ratio were calculated to gain further insight in the comparison of the accuracy of the two radiographic modalities for the detection of VRFs. Ideally, the positive likelihood ratio (LR+) should be as large as possible and the negative likelihood ratio (LR-) should be as small as possible. The results of this study showed that LR+ was significantly higher for periapical radiography than for CBCT. The LR+ is the ratio between the true positive rate and the false positive rate. The mean LR+ of 1.19 for CBCT implies that the probability of getting a positive test results when a fracture was present was only slightly greater than the probability of getting a positive test result when a fracture was not present. There was no statistically significant difference between the mean LR- values of the two modalities, although the mean LR- of CBCT was close to 1. In part, this can be contributed to the relative large standard deviations associated with the mean. However, both values were modest at best, indicating that the true negative rate (specificity) was offset by a sizable false negative rate. In other words, both a lack of specificity and a lack of sensitivity contributed to the weak LR- values.

Since the diagnostic odds ratio (DOR) is the ratio between the LR+ and the LR-, it is not surprising that the mean DOR of periapical radiography was significantly better than the mean DOR of CBCT. The mean DOR value of 3.52 for periapical radiography implies that the odds of a fracture being present when the test result is positive was 3.52 times higher than the odds of a fracture being present when the test result was negative. For CBCT, the odds of a fracture being present when the test result is positive was 1.77 times higher than the odds of a fracture being present when the test result was negative. This implies that the discriminatory power of CBCT for the detection of VRFs was weaker than the discriminatory power of periapical radiography.

Although the ROC analysis provides an overall measure of diagnostic accuracy, independent of prevalence and observers' individual decision thresholds, the additional measures of diagnostic accuracy provide insight into the underlying cause of limited diagnostic accuracy. It is acknowledged that the required dichotomization of the raw ROC scores adds an arbitrary element to the analysis, which slightly weakens its impact. Nevertheless, it was shown that both modalities were relatively weak with respect to the detection of fracture teeth, but that the difference between the modalities was largely based on difference in the false positive rate between the two modalities, with an overall lower discriminatory power of CBCT in this study.

One of the aims in designing this study was to develop a model that would resemble clinical conditions as closely as possible. Initially, a cadaver head was used, which would have been

an ideal model for this purpose. However, the manipulation of tissues and access to the sample teeth proved extremely difficult. Thus it was decided to use dry human skulls submerged in water. This model facilitate the manipulation of the sample teeth, while retaining the benefits of a complete anatomical model and the simulation of soft tissue induced scatter radiation.

The statistical analyses for each of the measures of diagnostic performance showed that there were no statistically significant differences between the observers for any of the measures. Although differences were present between individual observers, they appeared sufficiently homogenous for final analysis. While the eight observers had different backgrounds in terms of specialty and experience, it was not a goal to test whether there were differences between groups of observers. Instead, the aim was to use a homogenous group of observers bringing comparable skill sets to the study. As it was not possible to identify a group of volunteers with identical backgrounds in a single academic institution, the composition of the group was a convenience choice to some degree. The calibration of the observers and the statistical testing for difference provides some assurance that our assumptions about the observer group were justified.

The main reason for the experiment to be *in-vitro* rather than *in-vivo* was the necessity to have access to the ground truth. Ground truth in this study was established by intentionally inducing fractures and by verification of fractured and non-fractured teeth with 1%

methylene blue staining. The extent and orientation of the stained VRFs in each sample was recorded to confirm that each fracture was a true VRF.

All teeth intentionally fractured within this study were confirmed fractured through methylene blue staining and magnification. The extent of the fractures varied, but all teeth fractured contained non-displaced bucco-lingual fractures. Amongst the non-fractured control teeth, no fractures were observed along the roots in any orientation using the methylene blue staining. Although the same individual who fractured the teeth also stained and verified the teeth, the potential for systematic errors appears negligible. As the ground truth was established prior to the observation sessions, there was no opportunity for bias in the ground truth assessment.

Possible sources of bias were present in this study. Observers were able to freely manipulate CBCT images in terms of window and leveling (equivalent to contrast and brightness), whereas contrast and brightness could not be controlled for the three angled periapical radiographs for each sample. This potential bias could have favored CBCT, however, since the results of this study favor periapical radiography, concern about this potential bias is minimal. Some may argue, however, that the ability to freely manipulate images may actually reduce diagnostic accuracy because of a potential increase in the false positive rate. Although this theory cannot be refuted based on this study, it appears unlikely that the effect would be significant. However, only studies designed to test this theory will be able to

answer this question. It can also be argued that a bias was created to favor periapical radiography by using three angled radiographs for each sample, which is not advised clinically.

Another potential weakness of the study is the sample. Clearly, the prevalence of fractures in the sample (42%) was much larger than the prevalence of fractures in the population. The observers were informed about the purpose of the study, but not about the sample prevalence. This may have affected observer responses because they were unaware of the fracture prevalence within the sample group. Moreover, since the study was not clinical, information regarding clinical signs and symptoms could not be used in the diagnostic decision making process. Previous studies have shown that clinically, radiographic pathology associated with VRFs has aided in their diagnosis. Radiographic visualization of periapical pathology, bone loss and resorption in association with a VRF has been used in detection [64-68]. In this study, the results only represent the ability of the diagnostic modality to depict and the ability of the observer to identify a fractured root or a non-fractured root. It could be argued that the clinical diagnostic accuracy of CBCT could be higher than the accuracy obtained in this study, because of the potential detection of radiographic signs associated with VRFs.

Finally, this study only included one CBCT scanner. The Sirona Galileos Comfort was used, in part because it was available for the study and in part because it is one of the more popular scanners being sold in the United Sates. The Galileos uses a medium size field of view and is not specifically designed for diagnostic tasks requiring high spatial resolution. On the other

hand, the ability to unbind voxels and use the native voxel size of 0.15 mm suggests that the Galileos could be used for such tasks. It should be emphasized that the results of this study apply to the Sirona Galileos Comfort unit only and cannot be generalized to other CBCT scanners. It could be argued that CBCT scanner with comparable fields of view and resolution may yield similar results. However, there are CBCT units on the market that use a smaller field of view, likely with higher contrast and spatial resolutions. Examples include the Kodak 9000 3D, Morita 3D Accuitomo FPD, Planmeca Promax 3D s and the TeraRecon PreXion. It is reasonable to assume that CBCT scanners with a limited field of view and higher resolution are more likely to be more accurate for the detection of VRFs. Future studies should include these scanners and assess their usefulness in endodontic and general dental diagnostic decision making.

Based on the results of this study it is concluded that:

1. Periapical radiographs are more accurate than the Sirona Galileos Comfort CBCT scanner for the detection of vertical root fractures.
2. The specificity, the positive likelihood ratio and the diagnostic odds ratio are better for periapical radiography
3. The sensitivity and negative likelihood ratio of periapical radiography and CBCT are not different.
4. The differences between the two modalities are largely the result of a higher false positive rate associated with CBCT.

REFERENCES

1. Rivera, E.M. and A. Williamson, *Diagnosis and treatment planning: cracked tooth.* Tex Dent J, 2003. **120**(3): p. 278-83.

2. Rivera, E.M. and R.E. Walton, *Longitudinal tooth fractures,* in *Principles and practice of endodontics,* M. Torabinejad and R.E. Walton, Editors. 2009, W.B. Saunders Company: Philadelphia, Pennsylvania. p. 108-128.

3. Rivera, E.M. and R.E. Walton, *Cracking the cracked tooth code: detection and treatment of various longitudinal tooth fractures.* American Association of Endodontists Colleagues for Excellence, 2008. **Summer**.

4. Rivera, E.M. and R.E. Walton, *Longitudinal tooth fractures: findings that contribute to complex endodontic diagnoses.* Endodontic Topics, 2009. **16**(1): p. 82-111.

5. Abou-Rass, M., *Crack lines: the precursors of tooth fractures - their diagnosis and treatment.* Quintessence Int Dent Dig, 1983. **14**(4): p. 437-47.

6. Gher, M.E., Jr., et al., *Clinical survey of fractured teeth.* J Am Dent Assoc, 1987. **114**(2): p. 174-7.

7. Opdam, N.J. and J.M. Roeters, *The effectiveness of bonded composite restorations in the treatment of painful, cracked teeth: six-month clinical evaluation.* Oper Dent, 2003. **28**(4): p. 327-33.

8. Cohen, S., et al., *A demographic analysis of vertical root fractures.* J Endod, 2006. **32**(12): p. 1160-3.

9. Rosen, H., *Cracked tooth syndrome.* J Prosthet Dent, 1982. **47**(1): p. 36-43.

10. Schweitzer, J.L., J.L. Gutmann, and R.Q. Bliss, *Odontiatrogenic tooth fracture.* Int Endod J, 1989. **22**(2): p. 64-74.

11. Ellis, S.G., *Incomplete tooth fracture--proposal for a new definition.* Br Dent J, 2001. **190**(8): p. 424-8.

12. Lynch, C.D. and R.J. McConnell, *The cracked tooth syndrome.* J Can Dent Assoc, 2002. **68**(8): p. 470-5.

13. Cavel, W.T., W.P. Kelsey, and R.J. Blankenau, *An in vivo study of cuspal fracture.* J Prosthet Dent, 1985. **53**(1): p. 38-42.

14. Lagouvardos, P., P. Sourai, and G. Douvitsas, *Coronal fractures in posterior teeth.* Oper Dent, 1989. **14**(1): p. 28-32.

15. Cohen, S., L. Blanco, and L. Berman, *Vertical root fractures: clinical and radiographic diagnosis.* J Am Dent Assoc, 2003. **134**(4): p. 434-41.

16. Fennis, W.M., et al., *A survey of cusp fractures in a population of general dental practices.* Int J Prosthodont, 2002. **15**(6): p. 559-63.

17. Silvestri, A.R., Jr. and I. Singh, *Treatment rationale of fractured posterior teeth.* J Am Dent Assoc, 1978. **97**(5): p. 806-10.

18. Hiatt, W.H., *Incomplete crown-root fracture in pulpal-periodontal disease.* J Periodontol, 1973. **44**(6): p. 369-79.

19. Cameron, C.E., *Cracked-Tooth Syndrome.* J Am Dent Assoc, 1964. **68**: p. 405-11.

20. Cameron, C.E., *The cracked tooth syndrome: additional findings.* J Am Dent Assoc, 1976. **93**(5): p. 971-5.

21. Eakle, W.S., E.H. Maxwell, and B.V. Braly, *Fractures of posterior teeth in adults.* J Am Dent Assoc, 1986. **112**(2): p. 215-8.

22. Roh, B.D. and Y.E. Lee, *Analysis of 154 cases of teeth with cracks.* Dent Traumatol, 2006. **22**(3): p. 118-23.

23. Krell, K.V. and E.M. Rivera, *A six year evaluation of cracked teeth diagnosed with reversible pulpitis: treatment and prognosis.* J Endod, 2007. **33**(12): p. 1405-7.

24. Brynjulfsen, A., et al., *Incompletely fractured teeth associated with diffuse longstanding orofacial pain: diagnosis and treatment outcome.* Int Endod J, 2002. **35**(5): p. 461-6.

25. Abbott, P.V., *Assessing restored teeth with pulp and periapical diseases for the presence of cracks, caries and marginal breakdown.* Aust Dent J, 2004. **49**(1): p. 33-9; quiz 45.

26. Blaser, P.K., et al., *Effect of designs of Class 2 preparations on resistance of teeth to fracture.* Oper Dent, 1983. **8**(1): p. 6-10.

27. Stewart, G.G., *The detection and treatment of vertical root fractures.* J Endod, 1988. **14**(1): p. 47-53.

28. Reeh, E.S., H.H. Messer, and W.H. Douglas, *Reduction in tooth stiffness as a result of endodontic and restorative procedures.* J Endod, 1989. **15**(11): p. 512-6.

29. Ailor, J.E., Jr., *Managing incomplete tooth fractures.* J Am Dent Assoc, 2000. **131**(8): p. 1168-74.

30. Maxwell, E.H. and B.V. Braly, *Incomplete tooth fracture. Prediction and prevention.* CDA J, 1977. **5**(6): p. 51-5.

31. Pitts, D.L. and E. Natkin, *Diagnosis and treatment of vertical root fractures.* J Endod, 1983. **9**(8): p. 338-46.

32. Tamse, A., et al., *An evaluation of endodontically treated vertically fractured teeth.* J Endod, 1999. **25**(7): p. 506-8.

33. Pitts, D.L., H.E. Matheny, and J.I. Nicholls, *An in vitro study of spreader loads required to cause vertical root fracture during lateral condensation.* J Endod, 1983. **9**(12): p. 544-50.

34. Ricks-Williamson, L.J., et al., *A three-dimensional finite-element stress analysis of an endodontically prepared maxillary central incisor.* J Endod, 1995. **21**(7): p. 362-7.

35. Lustig, J.P., A. Tamse, and Z. Fuss, *Pattern of bone resorption in vertically fractured, endodontically treated teeth.* Oral Surg Oral Med Oral Pathol Oral Radiol Endod, 2000. **90**(2): p. 224-7.

36. Lertchirakarn, V., J.E. Palamara, and H.H. Messer, *Patterns of vertical root fracture: factors affecting stress distribution in the root canal.* J Endod, 2003. **29**(8): p. 523-8.

37. Lam, P.P., J.E. Palamara, and H.H. Messer, *Fracture strength of tooth roots following canal preparation by hand and rotary instrumentation.* J Endod, 2005. **31**(7): p. 529-32.

38. Tamse, A., *Iatrogenic vertical root fractures in endodontically treated teeth.* Endod Dent Traumatol, 1988. **4**(5): p. 190-6.

39. Meister, F., Jr., T.J. Lommel, and H. Gerstein, *Diagnosis and possible causes of vertical root fractures.* Oral Surg Oral Med Oral Pathol, 1980. **49**(3): p. 243-53.

40. Harvey, T.E., J.T. White, and I.J. Leeb, *Lateral condensation stress in root canals.* J Endod, 1981. **7**(4): p. 151-5.

41. Obermayr, G., et al., *Vertical root fracture and relative deformation during obturation and post cementation.* J Prosthet Dent, 1991. **66**(2): p. 181-7.

42. Tamse, A., et al., *Radiographic features of vertically fractured, endodontically treated maxillary premolars.* Oral Surg Oral Med Oral Pathol Oral Radiol Endod, 1999. **88**(3): p. 348-52.

43. Rud, J. and K.A. Omnell, *Root fractures due to corrosion. Diagnostic aspects.* Scand J Dent Res, 1970. **78**(5): p. 397-403.

44. Ross, R.S., J.I. Nicholls, and G.W. Harrington, *A comparison of strains generated during placement of five endodontic posts.* J Endod, 1991. **17**(9): p. 450-6.

45. Harrington, G.W., *The perio-endo question: differential diagnosis.* Dent Clin North Am, 1979. **23**(4): p. 673-90.

46. Tamse, A., et al., *Radiographic features of vertically fractured endodontically treated mesial roots of mandibular molars.* Oral Surg Oral Med Oral Pathol Oral Radiol Endod, 2006. **101**(6): p. 797-802.

47. Kurtzman, G.M., L.H. Silverstein, and P.C. Shatz, *Hemisection as an alternative treatment for vertically fractured mandibular molars.* Compend Contin Educ Dent, 2006. **27**(2): p. 126-9.

48. Nair, M.K., et al., *Detection of artificially induced vertical radicular fractures using tuned aperture computed tomography.* Eur J Oral Sci, 2001. **109**(6): p. 375-9.

49. Youssefzadeh, S., et al., *Dental vertical root fractures: value of CT in detection.* Radiology, 1999. **210**(2): p. 545-9.

50. Hannig, C., et al., *Three-dimensional, non-destructive visualization of vertical root fractures using flat panel volume detector computer tomography: an ex vivo in vitro case report.* Int Endod J, 2005. **38**(12): p. 904-13.

51. Mora, M.A., et al., *In vitro assessment of local computed tomography for the detection of longitudinal tooth fractures.* Oral Surg Oral Med Oral Pathol Oral Radiol Endod, 2007. **103**(6): p. 825-9.

52. Mora, M.A., et al., *Effect of the number of basis images on the detection of longitudinal tooth fractures using local computed tomography.* Dentomaxillofac Radiol, 2007. **36**(7): p. 382-6.

53. Scarfe, W.C. and A.G. Farman, *Cone-beam computed tomography,* in *Oral Radiology: Principles and Interpretation*, S.C. White and M.J. Pharoah, Editors. 2009, Mosby/Elsevier: St. Louis, MO. p. 225-244.

54. Robb, R.A., *The Dynamic Spatial Reconstructor: An X-Ray Video-Fluoroscopic CT Scanner for Dynamic Volume Imaging of Moving Organs.* IEEE Trans Med Imaging, 1982. **1**(1): p. 22-33.

55. Scarfe, W.C., A.G. Farman, and P. Sukovic, *Clinical applications of cone-beam computed tomography in dental practice.* J Can Dent Assoc, 2006. **72**(1): p. 75-80.

56. Scarfe, W.C. and A.G. Farman, *What is cone-beam CT and how does it work?* Dent Clin North Am, 2008. **52**(4): p. 707-30, v.

57. Scaf, G., et al., *Dosimetry and cost of imaging osseointegrated implants with film-based and computed tomography.* Oral Surg Oral Med Oral Pathol Oral Radiol Endod, 1997. **83**(1): p. 41-8.

58. Schulze, D., et al., *Radiation exposure during midfacial imaging using 4- and 16-slice computed tomography, cone beam computed tomography systems and conventional radiography.* Dentomaxillofac Radiol, 2004. **33**(2): p. 83-6.

59. Dula, K., et al., *Hypothetical mortality risk associated with spiral computed tomography of the maxilla and mandible.* Eur J Oral Sci, 1996. **104**(5-6): p. 503-10.

60. Hassan, B., et al., *Detection of vertical root fractures in endodontically treated teeth by a cone beam computed tomography scan.* J Endod, 2009. **35**(5): p. 719-22.

61. Hassan, B., et al., *Comparison of five cone beam computed tomography systems for the detection of vertical root fractures.* J Endod, 2010. **36**(1): p. 126-9.

62. Monaghan, P., et al., *A method for producing experimental simple vertical root fractures in dog teeth.* J Endod, 1993. **19**(10): p. 512-5.

63. Ludlow, J.B., et al., *Accuracy of measurements of mandibular anatomy in cone beam computed tomography images.* Oral Surg Oral Med Oral Pathol Oral Radiol Endod, 2007. **103**(4): p. 534-42.

64. Nair, M.K. and U.P. Nair, *Digital and advanced imaging in endodontics: a review.* J Endod, 2007. **33**(1): p. 1-6.

65. Misch, K.A., E.S. Yi, and D.P. Sarment, *Accuracy of cone beam computed tomography for periodontal defect measurements.* J Periodontol, 2006. **77**(7): p. 1261-6.

66. Mol, A. and A. Balasundaram, *In vitro cone beam computed tomography imaging of periodontal bone.* Dentomaxillofac Radiol, 2008. **37**(6): p. 319-24.

67. Patel, S., et al., *The potential applications of cone beam computed tomography in the management of endodontic problems.* Int Endod J, 2007. **40**(10): p. 818-30.

68. Lofthag-Hansen, S., et al., *Limited cone-beam CT and intraoral radiography for the diagnosis of periapical pathology.* Oral Surg Oral Med Oral Pathol Oral Radiol Endod, 2007. **103**(1): p. 114-9.

Appendix I:
Tables

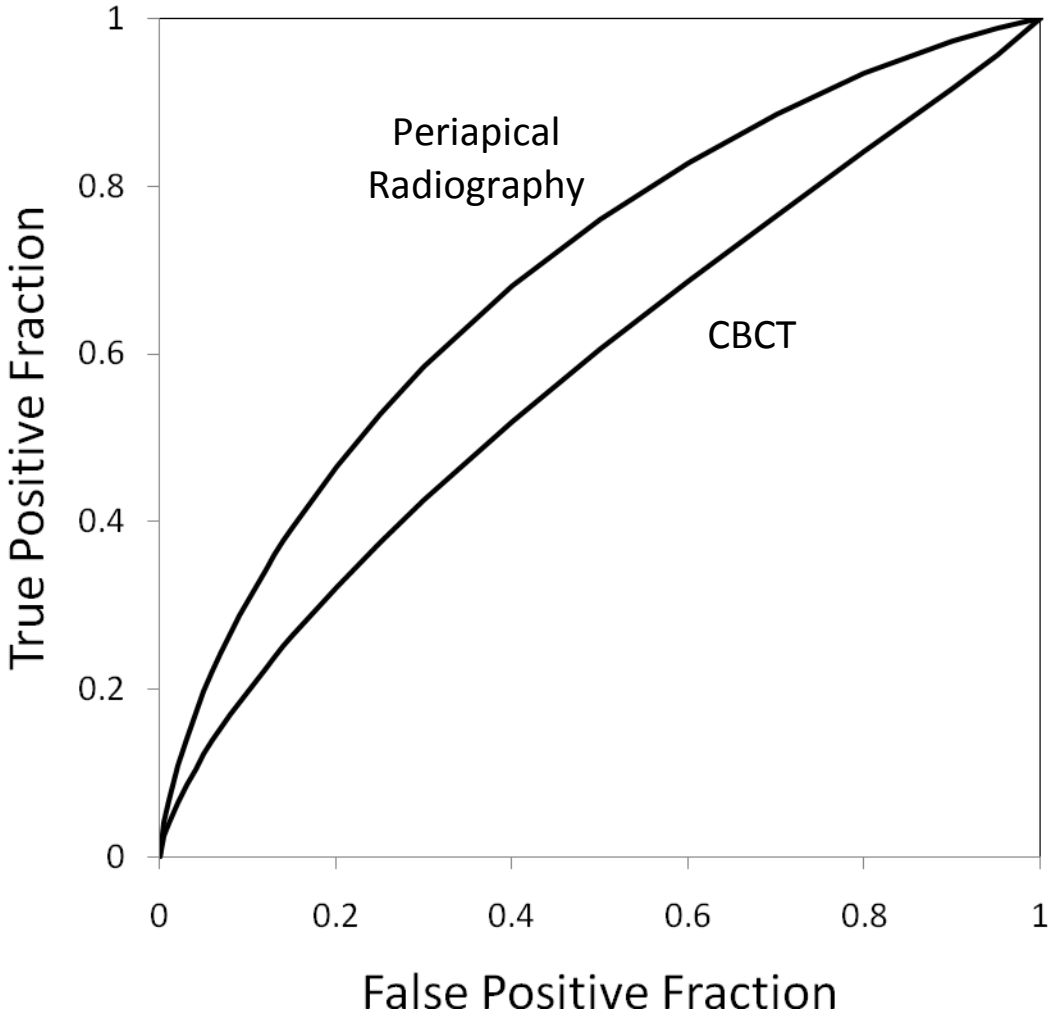

Figure 1. ROC Curve. Receiver operating characteristic curves based on pooled data for periapical radiography (A_z = 0.70) and CBCT (A_z= 0.58)

Table 1. Sample

Teeth	Fractured	Non-fractured
Mandibular premolar	6	5
Maxillary premolar	4	6
Mandibular molar	5	8
Maxillary molar	6	10
Total	21	29

Table 2. ROC A_z-values for vertical root fracture detection

Observer	Periapical Radiography	CBCT
1	0.73	0.57
2	0.70	0.66
3	0.57	0.65
4	0.66	0.47
5	0.78	0.66
6	0.62	0.48
7	0.77	0.52
8	0.74	0.63
Mean	0.70	0.58
SD	0.07	0.08

ANOVA: modality: p = 0.0134; observer: p = 0.3307

Table 3. Sensitivity for vertical root fracture detection

Observer	Periapical Radiography	CBCT
1	0.57	0.90
2	0.57	0.67
3	0.57	0.71
4	0.43	0.38
5	0.52	0.71
6	0.38	0.33
7	0.67	0.48
8	0.62	0.62
Mean	0.54	0.60
SD	0.10	0.19

ANOVA: modality: $p = 0.3445$; observer: $p = 0.1360$

Table 4. Specificity for vertical root fracture detection

Observer	Periapical Radiography	CBCT
1	0.72	0.24
2	0.76	0.59
3	0.55	0.45
4	0.72	0.59
5	0.76	0.28
6	0.90	0.62
7	0.69	0.52
8	0.69	0.62
Mean	0.72	0.49
SD	0.10	0.15

ANOVA: modality: p = 0.0048; observer: p = 0.3181

Table 5. Positive likelihood ratio for vertical root fracture detection

Observer	Periapical Radiography	CBCT
1	2.07	1.19
2	2.37	1.61
3	1.27	1.29
4	1.55	0.92
5	2.17	0.99
6	3.68	0.88
7	2.15	0.99
8	1.99	1.63
Mean	2.16	1.19
SD	0.71	0.20

ANOVA: modality: p = 0.0139; observer: p = 0.6839

Table 6. Negative likelihood ratio for vertical root fracture detection

Observer	Periapical Radiography	CBCT
1	0.59	0.39
2	0.56	0.57
3	0.78	0.64
4	0.79	1.06
5	0.63	1.04
6	0.69	1.07
7	0.48	1.01
8	0.55	0.61
Mean	0.63	0.80
SD	0.11	0.27

ANOVA: modality: $p = 0.1286$; observer: $p = 0.3456$

Table 7. Diagnostic odds ratio for vertical root fracture detection

Observer	Periapical Radiography	CBCT
1	3.50	3.02
2	4.19	2.83
3	1.64	2.03
4	1.97	0.87
5	3.46	0.95
6	5.33	0.82
7	4.44	0.97
8	3.61	2.66
Mean	3.52	1.77
SD	1.23	0.97

ANOVA: modality: $p = 0.0189$; observer: $p = 0.587$

Appendix II:

Figures

Figure 2. Fractured Cusp

Figure 3. Cracked Tooth

Figure 4. Split Tooth

Figure 5. Vertical Root Fracture

Figure 6. Sirona Galileos Comfort

Figure 7. Sirona Galileos Comfort

Figure 8. Dry Skulls

Figure 9. Accessed Samples

Figure 10. Fracture Induction

Figure 11. Conical wedge and Mallet

Figure 12. Conical wedge

Figure 13. Ground Truth

Appendix III:
Radiographic Images

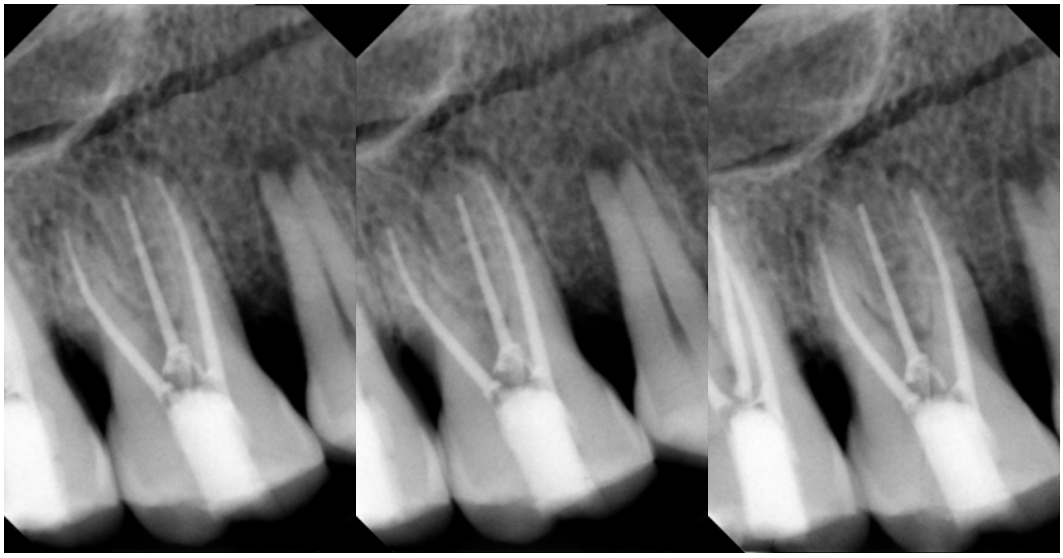

Figure 14. Multi-angled periapical Radiographs

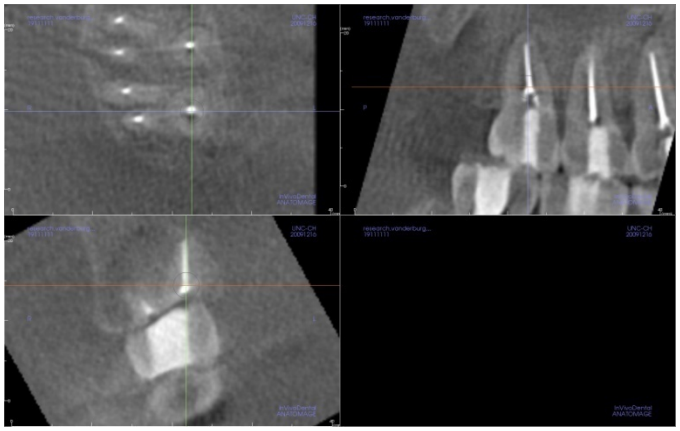

Figure 15. CBCT Scan

Figure 16. Periapical Radiograph

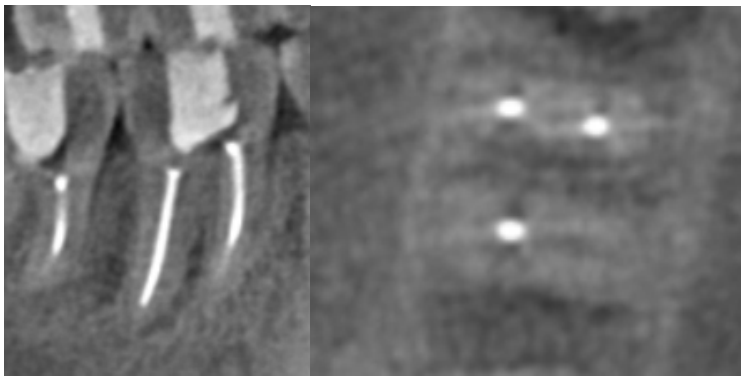

Figure 17. CBCT Reconstruction Image